Alma Mater Studiorum · University of Bologna

Visual Inspection of Motorcycle Connecting Rods [1]

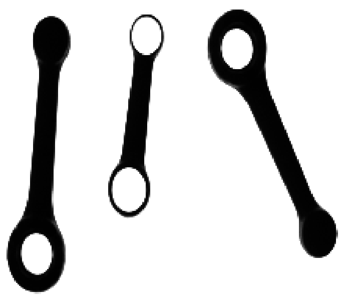

91277 - Project Work in Image Processing and Computer Vision
Project 11 - A.Y. 2021-22

Giuseppe Murro

Università di Bologna
giuseppe.murro@studio.unibo.it

October 20, 2022

[1]The code for the project is publicly available on GitHub

Contents

1 Introduction

The project work goal is to develop a software system aimed at visual inspection of motorcycle connecting rods. The system aims to analyse the dimensions of two different types of connecting rods to allow a vision-guided robot to pick and sort rods based on their type and dimensions. The two connecting rod types are characterized by a different number of holes: Type A rods have one hole whilst Type B rods have two holes.

Images of connecting rods have been taken by the backlighting technique so to render rods easily distinguishable (i.e. much darker) from background.

For each image, the system must be able to detect the rods and for each of them determine the type, the dimesions and the position into the image.

2 Initial configuration

2.1 Environment and libraries

The project has been developed using Jupyter Notebook. The python interpreter used is *python 3.5.6*, installed through Anaconda enviroment. The libraries used are the following:

- *numpy* version 1.18.5
- *matplotlib* version 3.0.3
- *opencv* version 3.4.2.16
- *scipy* version 1.4.1

All intermediate processings of the images are stored into a dictionary for each task, in order to be able to visualize them in the notebook and retrive them for further operations.

3 First task

The first task consists in inspecting a set of six images, where the connecting rods appear well separated and do not contain any distracting elements. Each image contains two or three connecting rods, which can be of both types and feature significantly diverse dimensions.

3.1 Histogram analysis

The first step is to analyse the histogram of the images. The histogram is a representation of the distribution of the pixel values in an image.

Since the images are in grayscale, the histogram is a plot of the number of pixels for each possible value in the range $[0, 255]$.

As can be seen from the histograms in Figure 3.1, the images are clearly bimodal, even if the peak of the second mode, corresponding to the background, is not very sharp due to light conditions.

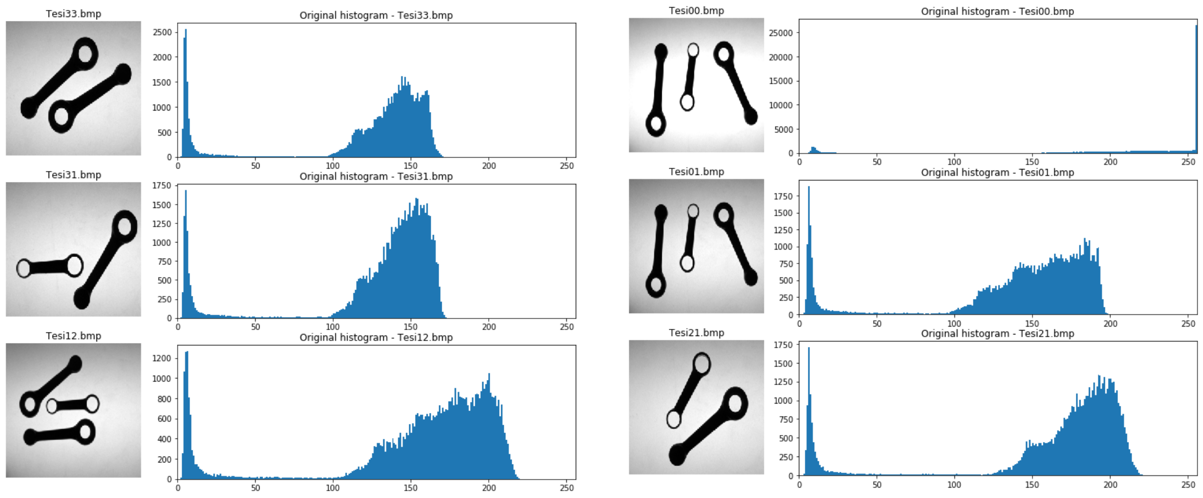

Figure 3.1: Histogram of original images from the first task

3.2 Image denoising

It is a good practice to denoise the images before performing any other operation. This is because the denoising process can remove some noise and improve the binarization.

The denoising process is performed using a linear trasformation like Gaussian Filter through `cv2.GaussianBlur()` function. Images are smoothed using kernel size of $3x3$. It is a discretization of the Gaussian function with a small σ (`sigma = 0.3*((ksize-1)*0.5 - 1) + 0.8` from opencv docs).

The Figure 3.2 shows the results of the denoising process. The images obtained are lightly smoother and the background is more homogeneous.

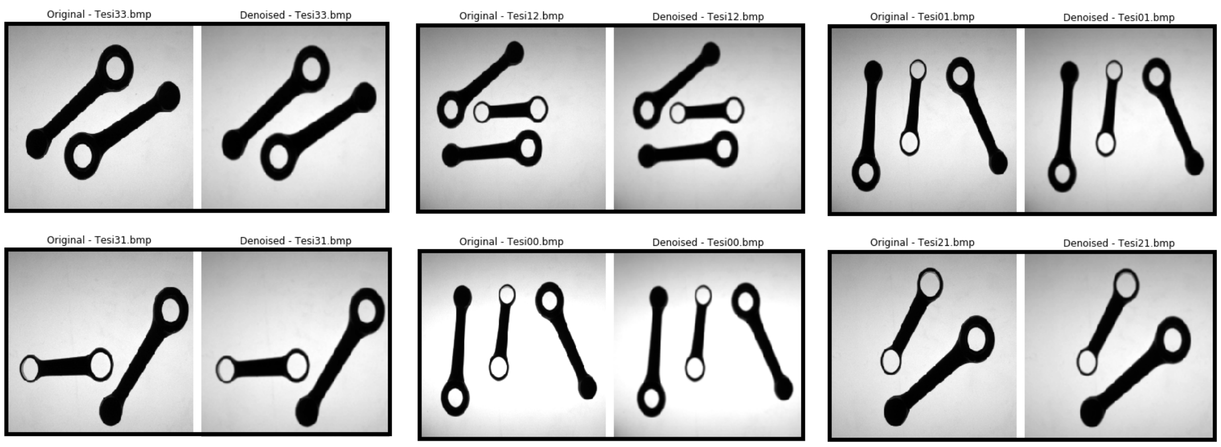

Figure 3.2: Denoising of original images from the first task

3.3 Binary segmentation

Since the images are bimodal, it is possible to perform a binary segmentation. The smoothing process improved the histograms and allows for a more correct binarization.

The binarization is performed using the Otsu' Algorithm (`cv2.threshold(img, 0, 255, cv2.THRESH_BINARY_INV |cv2.THRESH_OTSU)`. It is a theoretically based method for automatically choosing the threshold value for a binarized image.

The Figure 3.3 shows the results of the binarization process. At first glance, the obtained binary images are good, indeed they do not present false positives or false negatives.

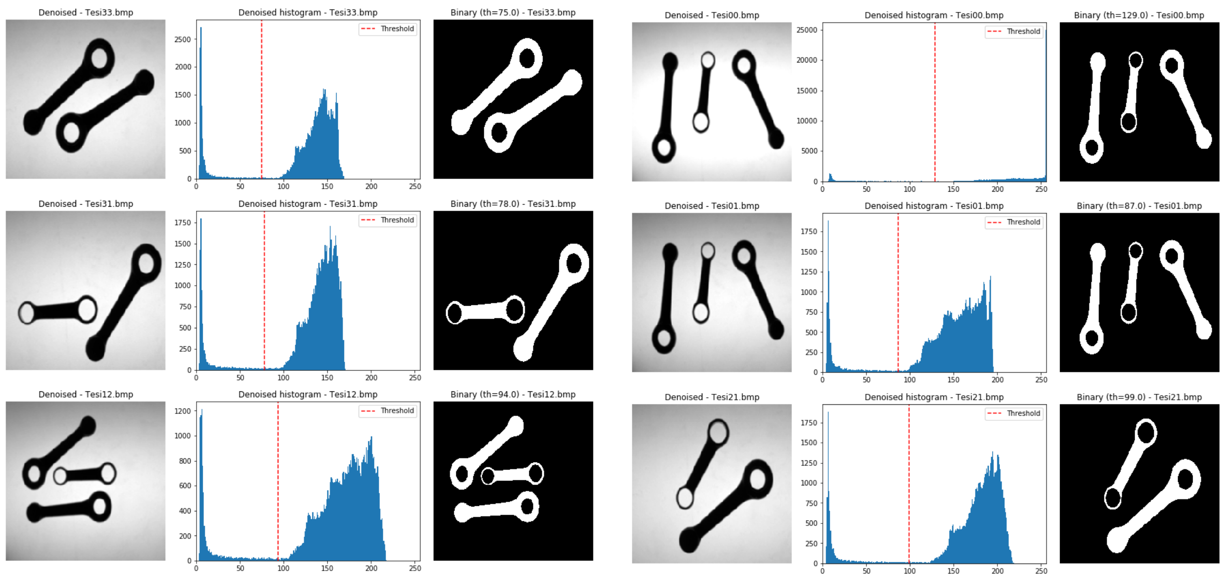

Figure 3.3: Binarization of denoised images from the first task

3.4 Connected components analysis

At this point, the foreground regions are further splitted into subregions corresponding to individual connecting rods. This is done performing a connected components analysis: pixels belonging to different objects are assigned different labels.

Using the `cv2.connectedComponentsWithStats()` function, it is possible to obtain the following information for each image:

- **Number of labels**: the number of connected components found in the image
- **Labels matrix**: a matrix of the same size of the image, where each pixel is assigned a label
- **Stats matrix**: a list of N bounding boxes, where N is the number of labels
- **Centroids matrix**: a list of N centroids, where N is the number of labels

The obtained objects are shown in Figure 3.4. The number of labels is correct for all images, this means that the connected components analysis is working correctly.

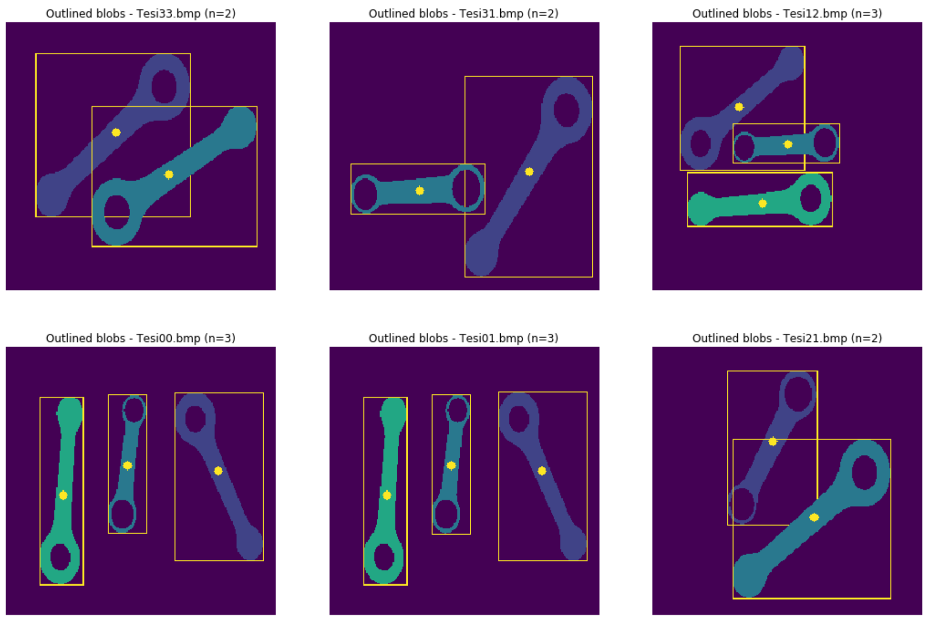

Figure 3.4: Connected component analysis of binary images from the first task

3.5 Blob inspection

For each connecting rod appearing in the image, the system provides the following information:

1. **Type**: the type of the connecting rod (A or B)
2. **Hole stats**: for each hole, position of the centre and diameter size
3. **Position**: the position of the barycentre of the blob
4. **Orientation**: the orientation of the connecting rod modulo π;
5. **Dimensions**: length and width of the minimum enclosing rectangle of the blob and the width at the barycenter

3.5.1 Type of rod detection

In order to detect the type of the connecting rod, the system count the number of holes in the blob. This could be easily done using the *Euler number* of the blob, which is the number of objects minus the number of holes. But since we want to assess that the holes are circles and we want measure statistics of them, Euler number is not a good choice.

A better approach is to use the `cv2.findContours()` function, which returns the contours of the foreground regions. So the number of holes is the number of contours minus one (the contour of the blob itself).

3.5.2 Holes stats

The position and the diameter of the holes are computed using the `get_holes_stats(contours, haralick_threshold=6)` function. The function takes as input the contours of the blob and the threshold for the Haralick circularity descriptor.

Only the contours with circularity greater than the threshold are considered as holes.

The diameter of the hole is computed with the following formula:

$$d = \sqrt{\frac{4 \cdot \text{area}}{\pi}} \tag{3.1}$$

3.5.3 Minimum enclosing rectangle

The minimum enclosing rectangle is computed using the `cv2.minAreaRect()` function applied to the blob contour. The *length* and *width* of the blob are respectively the bigger and the smaller side of the rectangle.

3.5.4 Orientation

The orientation of the blob is detemined as the angle θ between the major axis and the horizontal axis of the image reference system. To compute θ, it is necessary to minimize the following function :

$$M(\theta) = \sin^2(\theta)M'_{0,2} + 2\sin(\theta)\cos(\theta)M'_{1,1} + \cos^2(\theta)M'_{2,0} \tag{3.2}$$

where $M'_{i,j}$ is the i, j-th moment of the blob.

The zeros of the first derivative of $M(\theta)$ are θ_1 and θ_2, corresponding to the orientation of the major and minor axis of the blob:

$$\theta_1 = \frac{1}{2}\arctan\left(\frac{2M'_{1,1}}{M'_{0,2} - M'_{2,0}}\right) \qquad \text{and} \qquad \theta_2 = \frac{1}{2}\arctan\left(\frac{2M'_{1,1}}{M'_{0,2} - M'_{2,0}}\right) + \frac{\pi}{2} \tag{3.3}$$

To determine which one is relative to the major axis, it is necessary to analyze the second derivative of $M(\theta)$:

$$\frac{d^2M(\theta)}{d\theta^2} = \left(M'_{0,2} - M'_{2,0}\right) 2\cos(2\theta) + 4M'_{1,1}\sin(2\theta) \tag{3.4}$$

If $\frac{d^2M(\theta)}{d\theta^2}$ is negative, then θ_1 is the orientation of the major axis, otherwise $\theta_1 + \frac{\pi}{2}$ is the orientation of the major axis.

3.5.5 Width at barycentre

The barycenter of the blob is computed using the moments. The function `cv2.moments()` gives a dictionary of all moment values calculated. From these moments, the barycenter coordinates are given by the following relations:

$$C_x = \frac{M_{1,0}}{M_{0,0}} \qquad \text{and} \qquad C_y = \frac{M_{0,1}}{M_{0,0}} \tag{3.5}$$

Therefore the minor axis passing through the barycenter is given by the following formula:

$$y = mx + q \qquad \text{with} \qquad m = \tan(\theta_{min\_axis}) \qquad \text{and} \qquad q = C_y - mC_x \tag{3.6}$$

So the width at the barycenter is the distance between the two contour points that intersect the minor axis at the barycenter. It is computed by the `get_width_at_barycenter()` function.

3.5.6 Results

The results of the blob inspection are shown in Figure 3.5. The title of each image describe the relative informations. All the resulted values are correct and are consistent with an human inspection.

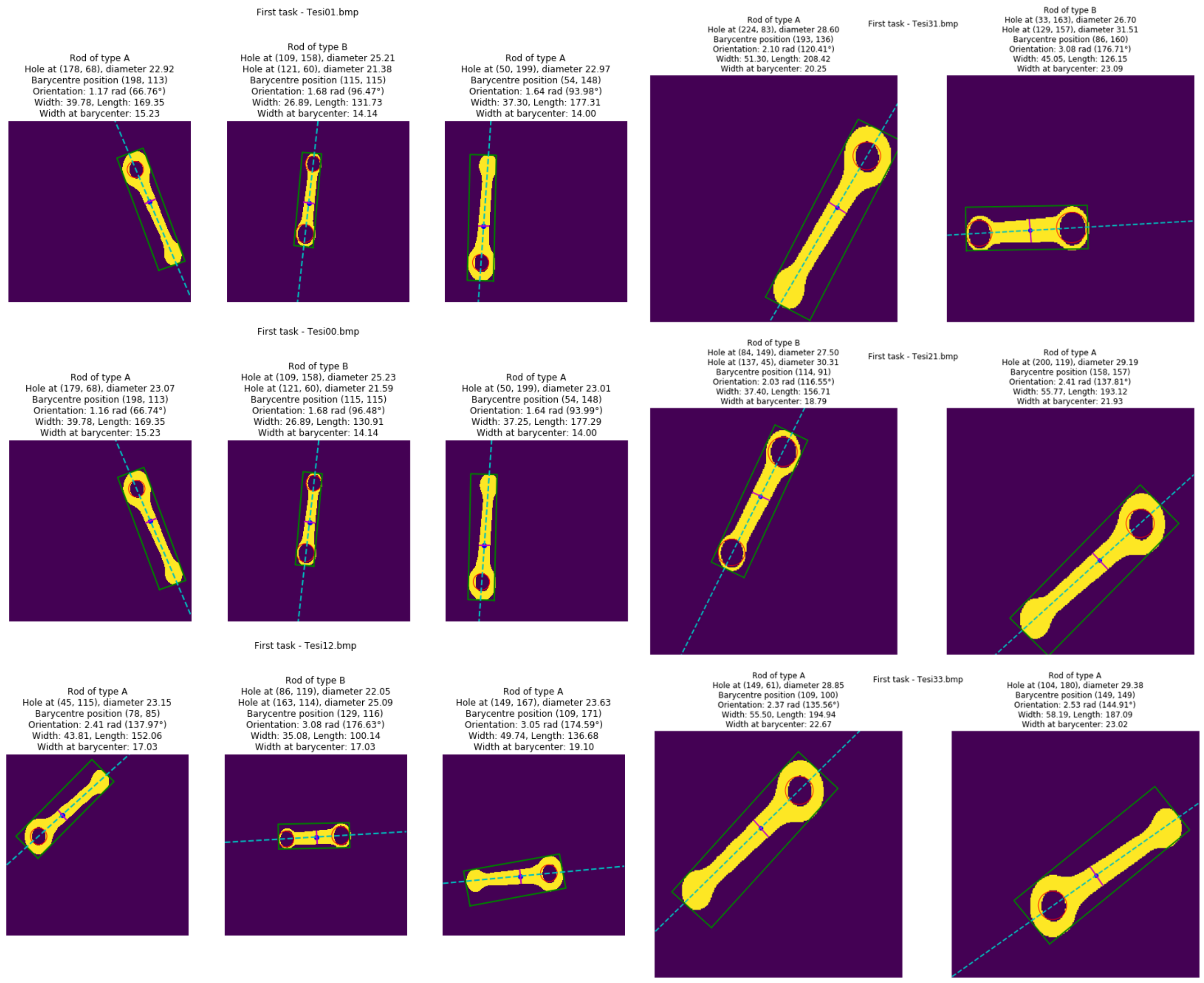
First task - Tesi01.bmp
Rod of type A
Hole at (178, 68), diameter 22.92
Barycentre position (198, 113)
Orientation: 1.17 rad (66.76°)
Width: 39.78, Length: 169.35
Width at barycenter: 15.23
Rod of type B
Hole at (109, 158), diameter 25.21
Hole at (121, 60), diameter 21.38
Barycentre position (115, 115)
Orientation: 1.68 rad (96.47°)
Width: 26.89, Length: 131.73
Width at barycenter: 14.14
Rod of type A
Hole at (50, 199), diameter 22.97
Barycentre position (54, 148)
Orientation: 1.64 rad (93.98°)
Width: 37.30, Length: 177.31
Width at barycenter: 14.00
First task - Tesi31.bmp
Rod of type A
Hole at (224, 83), diameter 28.60
Barycentre position (193, 136)
Orientation: 2.10 rad (120.41°)
Width: 51.30, Length: 208.42
Width at barycenter: 20.25
Rod of type B
Hole at (33, 163), diameter 26.70
Hole at (129, 157), diameter 31.51
Barycentre position (86, 160)
Orientation: 3.08 rad (176.71°)
Width: 45.05, Length: 126.15
Width at barycenter: 23.09
First task - Tesi00.bmp
Rod of type A
Hole at (179, 68), diameter 23.07
Barycentre position (198, 113)
Orientation: 1.16 rad (66.74°)
Width: 39.78, Length: 169.35
Width at barycenter: 15.23
Rod of type B
Hole at (109, 158), diameter 25.23
Hole at (121, 60), diameter 21.59
Barycentre position (115, 115)
Orientation: 1.68 rad (96.48°)
Width: 26.89, Length: 130.91
Width at barycenter: 14.14
Rod of type A
Hole at (50, 199), diameter 23.01
Barycentre position (54, 148)
Orientation: 1.64 rad (93.99°)
Width: 37.25, Length: 177.29
Width at barycenter: 14.00
First task - Tesi21.bmp
Rod of type B
Hole at (84, 149), diameter 27.50
Hole at (137, 45), diameter 30.31
Barycentre position (114, 91)
Orientation: 2.03 rad (116.55°)
Width: 37.40, Length: 156.71
Width at barycenter: 18.79
Rod of type A
Hole at (200, 119), diameter 29.19
Barycentre position (158, 157)
Orientation: 2.41 rad (137.81°)
Width: 55.77, Length: 193.12
Width at barycenter: 21.93
First task - Tesi12.bmp
Rod of type A
Hole at (45, 115), diameter 23.15
Barycentre position (78, 85)
Orientation: 2.41 rad (137.97°)
Width: 43.81, Length: 152.06
Width at barycenter: 17.03
Rod of type B
Hole at (86, 119), diameter 22.05
Hole at (163, 114), diameter 25.09
Barycentre position (129, 116)
Orientation: 3.08 rad (176.63°)
Width: 35.08, Length: 100.14
Width at barycenter: 17.03
Rod of type A
Hole at (149, 167), diameter 23.63
Barycentre position (109, 171)
Orientation: 3.05 rad (174.59°)
Width: 49.74, Length: 136.68
Width at barycenter: 19.10
First task - Tesi33.bmp
Rod of type A
Hole at (149, 61), diameter 28.85
Barycentre position (109, 100)
Orientation: 2.37 rad (135.56°)
Width: 55.50, Length: 194.94
Width at barycenter: 22.67
Rod of type A
Hole at (104, 180), diameter 29.38
Barycentre position (149, 149)
Orientation: 2.53 rad (144.91°)
Width: 58.19, Length: 187.09
Width at barycenter: 23.02

Figure 3.5: Visual inspection of images from the first task

4 Second task

While still meeting the requirement of the First Task, the system is modified in order to deal with a change in the characteristics of the working images. In particular, the system can now handle images such that the inspection area may be dirty due to the presence of scattered iron powder. The set of images that present those characteristics is composed by three pictures: `"Tesi90.bmp"`,`"Tesi92.bmp"`,`"Tesi98.bmp"`.

4.1 Image denoising adjusted

Since the images show a lot of impulse noise due to the presence of iron powder, it is necessary to apply a stronger smoothing step. A linear filter like the Gaussian filter is not enough, so a non-linear filter is used too. Purposely, a median filter with a kernel size of 3 is applied to the image before the Gaussian filter (`cv2.medianBlur()` function).

As can be seen in Figure 4.1, the median filter is able to remove most of the iron powder.

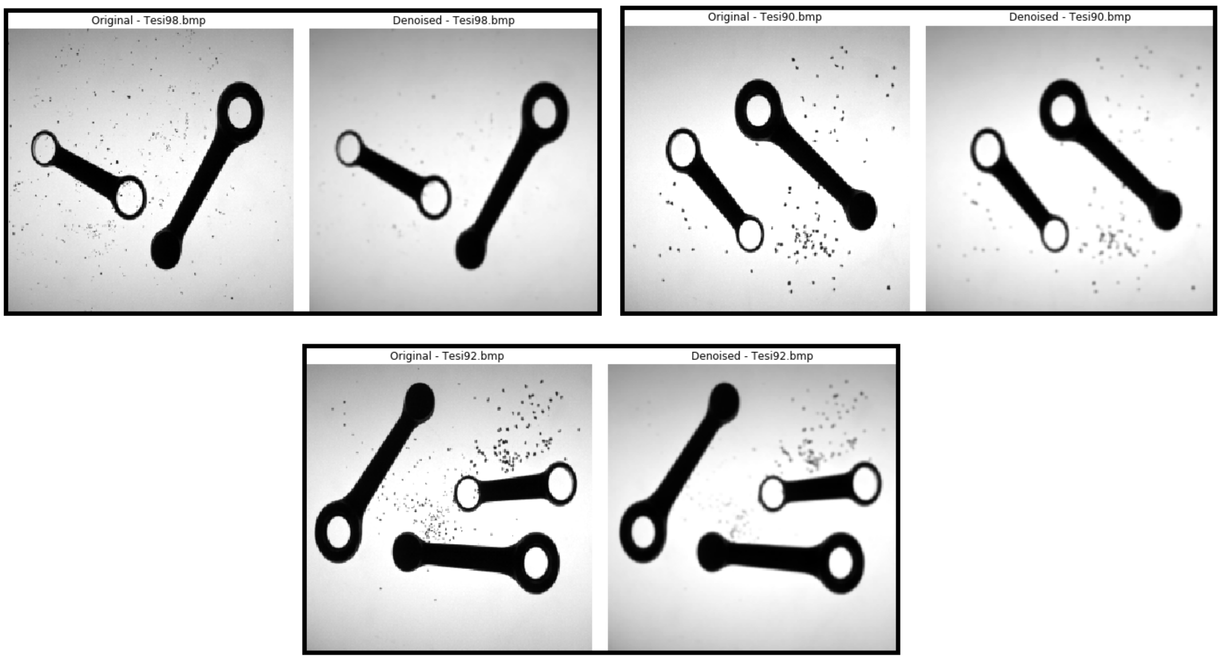

Figure 4.1: Denoising of original images from the second task

4.2 Filtered connected components

The naive connected component analysis performed on the first task is not enough to detect correctly the blobs in the images of the second task. Indeed a part of iron powder is still present in the images, and each granule would be detected as a blob.

Therefore a filtering step is added: the `connected_componentets_analysis()` function is redefined with an addictional parameter representing the minimum area of the blob. All the blobs with an area smaller than the minimum area (empirically set to 100) are discarded.

This small refinement allow to assign a correct label for each object, as shown in Figure 4.2.

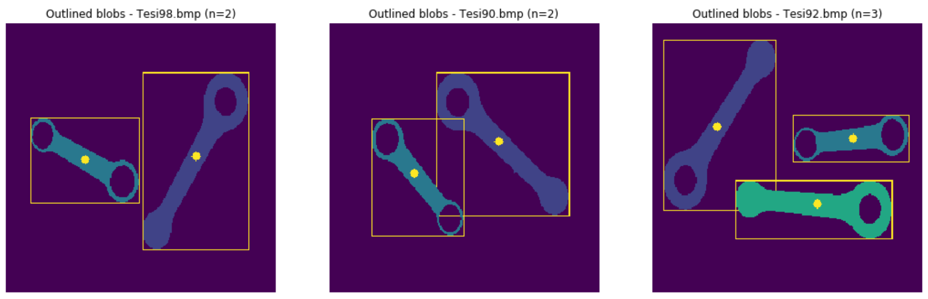
Outlined blobs - Tesi98.bmp (n=2)
Outlined blobs - Tesi90.bmp (n=2)
Outlined blobs - Tesi92.bmp (n=3)

Figure 4.2: Connected component analysis of binary images from the first task

4.3 Blob inspection

4.3.1 Results

The inspection of each blob is computed using the same `image_inspection()` function from the first task. A visual check of the results, in Figure 4.3, confirms that the inspection is correct.

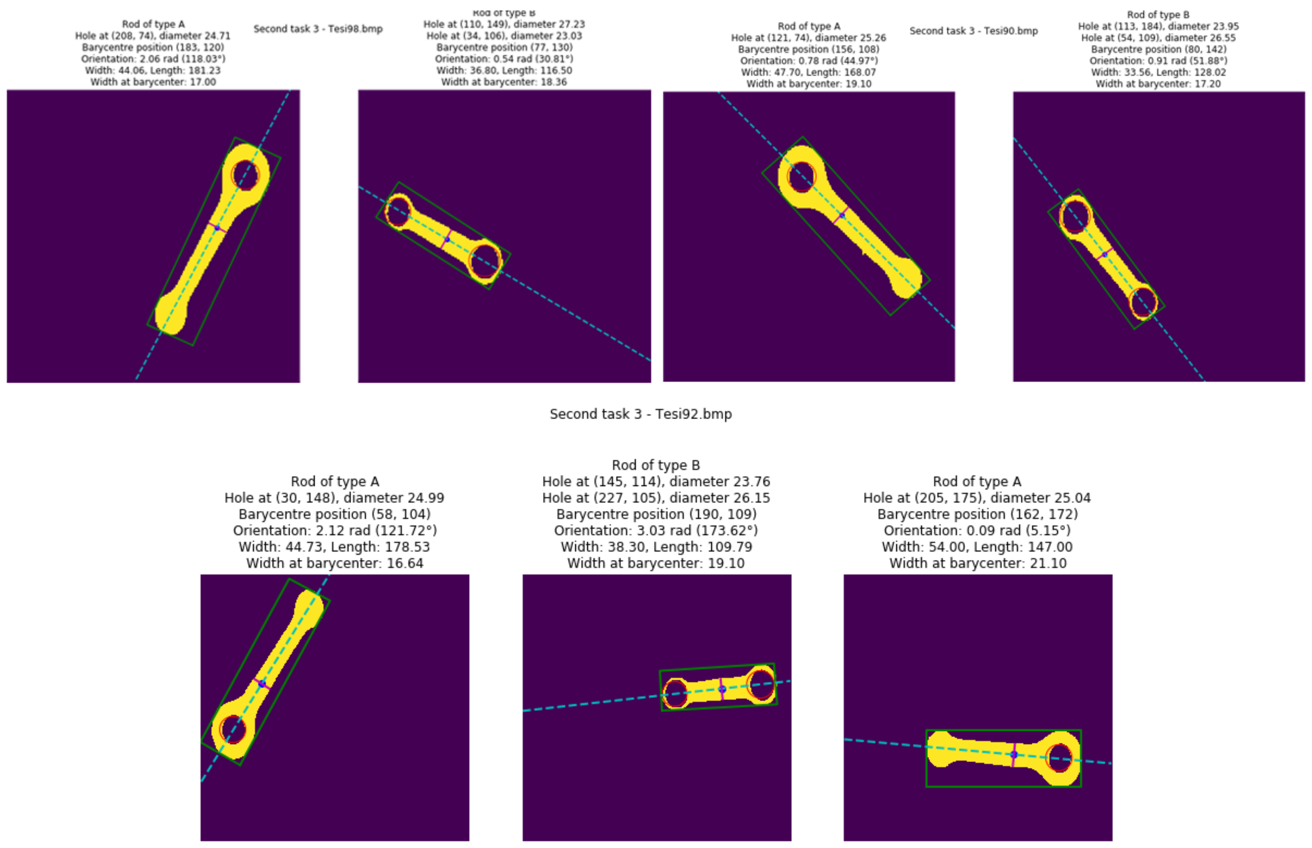
```
Second task 3 - Tesi98.bmp

Rod of type A
Hole at (208, 74), diameter 24.71
Barycentre position (183, 120)
Orientation: 2.06 rad (118.03°)
Width: 44.06, Length: 181.23
Width at barycenter: 17.00

Rod of type B
Hole at (110, 149), diameter 27.23
Hole at (34, 106), diameter 23.03
Barycentre position (77, 130)
Orientation: 0.54 rad (30.81°)
Width: 36.80, Length: 116.50
Width at barycenter: 18.36
```

```
Second task 3 - Tesi90.bmp

Rod of type A
Hole at (121, 74), diameter 25.26
Barycentre position (156, 108)
Orientation: 0.78 rad (44.97°)
Width: 47.70, Length: 168.07
Width at barycenter: 19.10

Rod of type B
Hole at (113, 184), diameter 23.95
Hole at (54, 109), diameter 26.55
Barycentre position (80, 142)
Orientation: 0.91 rad (51.88°)
Width: 33.56, Length: 128.02
Width at barycenter: 17.20
```

```
Second task 3 - Tesi92.bmp

Rod of type A
Hole at (30, 148), diameter 24.99
Barycentre position (58, 104)
Orientation: 2.12 rad (121.72°)
Width: 44.73, Length: 178.53
Width at barycenter: 16.64

Rod of type B
Hole at (145, 114), diameter 23.76
Hole at (227, 105), diameter 26.15
Barycentre position (190, 109)
Orientation: 3.03 rad (173.62°)
Width: 38.30, Length: 109.79
Width at barycenter: 19.10

Rod of type A
Hole at (205, 175), diameter 25.04
Barycentre position (162, 172)
Orientation: 0.09 rad (5.15°)
Width: 54.00, Length: 147.00
Width at barycenter: 21.10
```

Figure 4.3: Visual inspection of images from the second task